



Valorization of using agro-food waste as eco-friendly adsorbents for toxic dye removal from contaminated water

Rania M.A., Elshimaa H. Gomaa, Emam A.G,^{a,b} Elsis A.A

*Faculty of Science, Al-Azhar University (for girls), Yusuf Abbas street, Nasr city, Cairo, Egypt. Postal code: 11754 

Abstract

In this study, dried watermelon peels (DWP), an appropriate biological adsorbent, were employed to extract Acid Blue 193 (AB193) and Acid Orange 95 (AO95) from their aqueous solutions. These sorbents are affordable, safe for the environment, widely available, and very efficient. A variety of analysis, such as Scanning electron microscopy (SEM), Energy dispersive spectroscopy (EDX) and Fourier transform infrared (FTIR), have been used to determine the surface physicochemical properties before and after the adsorption process. In general, the characterization investigations showed that the adsorbent chemical structure contained several types of oxygenated functional groups and had a suitable shape for dye removal. Experimental work was done to identify the ideal working conditions, which were 60 min contact time, 0.3 g adsorbent mass, 30 °C, and pH= 3. This range of initial dye concentration was 25-150 ppm., and the percentage of removal reached to 97.99 % and 95.51 % for AB193 and AO95 respectively. The Freundlich model was found to provide a good fit to the data in terms of equilibrium, while the thermodynamic parameters suggested that the process was spontaneous and exothermic in nature. Additionally, kinetic tests showed that the acidic dyes removal rate followed a pseudo-second-order model, indicating that the adsorption was controlled by either intra-particle diffusion or diffusion on the stationary layer covering the adsorbent particles. Finally, the information gathered in this study supported the interest in using agricultural waste products as inexpensive lignocellulosic sorbents that could replace other pricey adsorbents in wastewater treatment.

Keywords: Acid Dyes ,Agro-food waste ;Bio-sorption; Dried watermelon peels;;water treatment.

1.Introduction

The rapid growth of the world's population and industrialization has already put pressure on natural resources which possess enormous challenges to the ecosystem [1]. Because the textile industry uses a large amount of water, global water resources are facing great pressure, so controlling water pollution is essential. Among the growing concerns of textile dyeing is the high consumption of water and the discharge of polluted water into the environment causing direct or indirect harmful effects on human health, aquatic life, and soils. Furthermore, they are considered carcinogens and must be processed before being released into water bodies [2].

Therefore, several dye-containing wastewater treatment methods have been developed and are currently being investigated and improved, such as oxidation, coagulation, electrochemical, biodegradation, and desorption processes [3]. The latter approach, in particular, is noteworthy for using adsorbents from agricultural residues as an economical and environmentally friendly method [4]. In order to remove dye, many low cost agricultural wastes are employed as adsorbents. Watermelon is

one of the heaviest and largest fruits, it is inexpensive and widely accessible [5–9], and its outer rind, a non-commercial offal, consists of a variety of substances, including proteins, citrullines, pectin, and carotenoids [10]. So in this study, one of the agricultural residues [agro-food waste (dried watermelon Peels)] that causes bad smell to the environment if left for some time was used as a natural sorbent that is available, inexpensive, highly effective and environmentally friendly because it was used without any chemical treatments.

2.Materials and methods

2.1Materials

All chemicals used during the investigation were analytical or laboratory-grade reagents. Distilled water was used for all experiments. dried watermelon peels (DWP), Acid Blue193 (AB193) , Acid Orange 95 (AO95) provided from the dyes factory tenth of Ramadan, Hydrochloric acid (0.1) N, sodium hydroxide (0.1) N and KNO₃ .

2.2. Methods

2.2.1 Watermelon peels collection and preparation

*Corresponding author e-mail: raniaamer845@gmail.com.; (Rania Mohamed Ahmed).

Receive Date: 01 April 2023, Revise Date: 30 April 2023, Accept Date: 15 May 2023

DOI: 10.21608/EJCHEM.2023.192762.7582

©2023 National Information and Documentation Center (NIDOC)

Watermelon peels were chosen as a biosorbent due to their wide availability, under-estimation, and eventual disposal as agricultural waste. Watermelon rinds were collected from leftover fruit shops throughout Cairo. After collection, the absorbent was rinsed thoroughly with distilled water to get rid of any residual water after being repeatedly washed with tap water to remove water-soluble contaminants, dust, dirt, etc. Finally, the cleaned and dried sorbent samples were spread out on filter papers and left in the shade to finish drying. It was then ground and sieved to produce a uniform volume of 1 μ . For later usage, the homogenate was kept in zip-top bags at room temperature [11].



Fig 1. Preparation of dried Watermelon peels

2.2.2 Characterization of dried watermelon peels (adsorbent)

The adsorbent before and after adsorption of the acid dyes onto the surface of the bio-adsorbent, DWP was characterized with Fourier Transform Infra Red Spectroscopy (FTIR) (JASCO FTIR 6100 spectrometer) and scanning electron microscopy (SEM) (a Quanta FEG 250 Czcch Republic electron microscope). Elemental analysis was performed using Energy-dispersive spectroscopy X-ray (EDX) (a Quanta FEG 250 Czcch Republic). The point- zero charge of DWP was determined by a digital pH meter (Satorius Model PB-11) and was used for other all experiments. pH_{pzc} is one of adsorbent characteristics. It was estimated by introducing 0.1 g of DWP in 50 mL of KNO_3 at initial pH values of (1-10) adjusted by adding required amounts of NaOH (0.1 N) or HCl (0.1 N). The mixture was stirred for 24 hours at room temperature, and the final pH was measured. When a graph of final pH verses (initial – final) pH was plotted and where the curve cuts X axis, these point is defined as pH_{pzc} [12].

2.2.3 Preparation of acid dyes stock solution (adsorbate)

AB193 [$C_{27}H_{34}N_2O_4S$] and AO95 [$C_{34}H_{28}N_4Na_2O_8S_2$] were purchased from New Trend Co. Egypt with molecular weight 482.62 and 730.72, respectively. To make a stock solution, 1 g of each dye powder was dissolved in 1 L of distilled water (1000 ppm). To establish the necessary experimental concentrations, the stock solution was diluted with distilled water. Final concentrations were determined

using 571 nm and 500 nm wavelength measurements, respectively using (Model T60, UK), UV-Visible spectrophotometer was used at a wavelength of 190-900 nm to record the absorbance of dye concentrations.

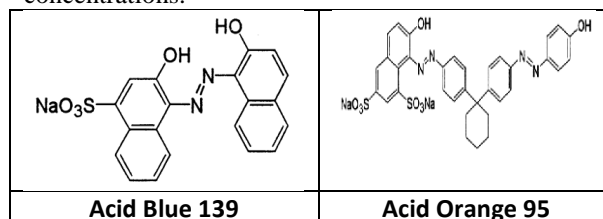


Fig 2. The chemical structure of the dyes.

2.2.4 Batch adsorption of acid dyes

The adsorption experiments were carried out in a batch process. The most important effective variables on adsorption include pH, adsorbent dose, contact time, temperatures and dye concentrations. Therefore, the initial acid dyes concentration was selected (25-150 ppm). The effect of adsorbent dosage (0.01- 0.4g/20ml of dye solution), contact time (0- 60 min) , pH (3-10) and temperature (10°C- 50°C) were studied. The experiments in batch system were carried out in a 50 ml Erlenmeyer flask Meyer. In every experiment, a certain concentration of acid dyes and specific dose of adsorbent spilled into the flask and completely mixed with shaker (Mettler waterbath, model WNB7-45, Germany) at 120 rpm for 60 minutes. Then the sample was filtrated. Spectrophotometer (Model T60, UK) residual concentrations were recorded at a maximum of 571 and 500 nm for AB13 and AO95, respectively [13, 14]. In the thermodynamic study, similar procedures were applied at (10 °C - 50 °C), with the other parameters held constant. the percentage of removal, R (%) of acid dyes were calculated using Equations (1)[15]. A Beer's law is applied to the dyes used and the drawing of the calibration curve, as shown in "Figure 3"

$$\text{Removal \%} = (C_0 - C_e / C_e) \times 100 \quad (1)$$

Where C_0 and C_e are initial and final concentrations of the dye in the solution respectively.

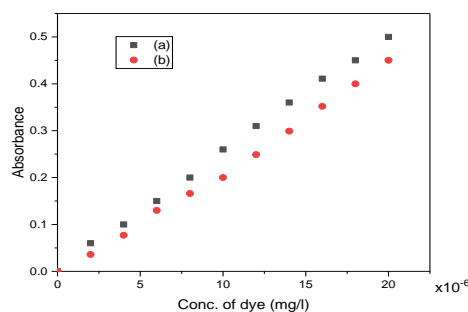


Fig. 3: Calibration curve of aqueous solutions of (a) AB193 (b) AO95 dyes



Fig 4. Image of dried watermelon peels before and after adsorption process.

3. Results and Discussion

3.1. Characterization of the dried watermelon peels as bio-sorbent (DWP)

3.1.1 Point zero charge (pHpzc) of the dried watermelon peels

Finding the pH at which the electrical charge on the surface of DWP was zero required determining the pH_{pzc} of DWP. The intersection between the first bisectrix and the curve representing the variation of the final pH with the initial pH gives a pH_{pzc}. "Figure 5" shows that the pH_{pzc} of DWP was at pH 4.7 which reflects the acidity of DWP. Since the surface of DWP is positively charged due to protonation, adsorption of anions is preferred at solution pH levels below the pH_{pzc} value, whereas adsorption of cations is preferred at solution pH levels above the pH_{pzc} value. In this regard, it is expected that the adsorption of the anionic AB193 and AO95 dyes by cationic DWP would be appropriate at pH of the solution is less than 4.7 due to electrostatic interactions [16].

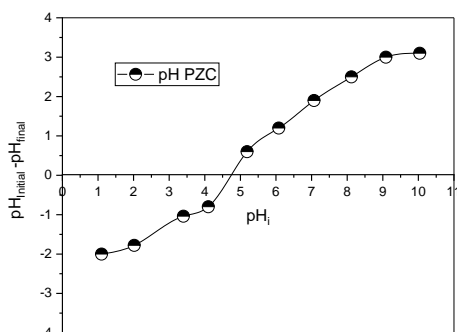


Fig. 5: Point zero charge of dried watermelon peels .

3.1.2 FTIR Spectrum Analysis

For determining the functional groups of any natural substance or synthetic chemical, FTIR spectroscopy is regarded as the most advanced technology. Functional groups present on the surface of DWP before and after the adsorption process were determined by using the FTIR spectrometer as shown in "Figure 6 a,b". According to the infrared spectrum of the DWP before adsorption of acid dyes, several strong, medium and weak bands appear as shown in "Figure 6a". which denote different functional groups, according to their waveform position (cm^{-1}) [17]. The wide and strong band at 3330 cm^{-1} is credited to the $-\text{OH}$ stretching vibrations of cellulose, pectin and lignin while the band at 2916 cm^{-1} corresponds to the $-\text{CH}$ stretching vibrations of the methyl group. The band at 1728 cm^{-1} indicates the $\text{C}=\text{O}$ stretching of carboxylic acid or esters. The asymmetric and symmetric vibrations of $-\text{COO}^-$ of the ionic carboxylic groups within DWP are represented by the band at 1622 and 1433 cm^{-1} , respectively. The IR bands between the 1300 and 1026 cm^{-1} region are assigned to the $\text{C}-\text{O}$ and $\text{C}-\text{O}-\text{C}$ stretching vibrations in carboxylic acids, alcohols, phenols or ester groups [18]. As indicated by the infrared spectrum of the DWP after AB193 and AO95 dyes uptake "Figure 6b", some bands shifted to about 1635 and 1617 cm^{-1} (bend-N-H) and 1234 and 1230 cm^{-1} (C-N vibration) denotes the interaction of AB193 and AO95 molecules respectively with the DWP functional groups. Moreover, the band intensities decreased during adsorption and this proves that the physical adsorption process took place [19,20].

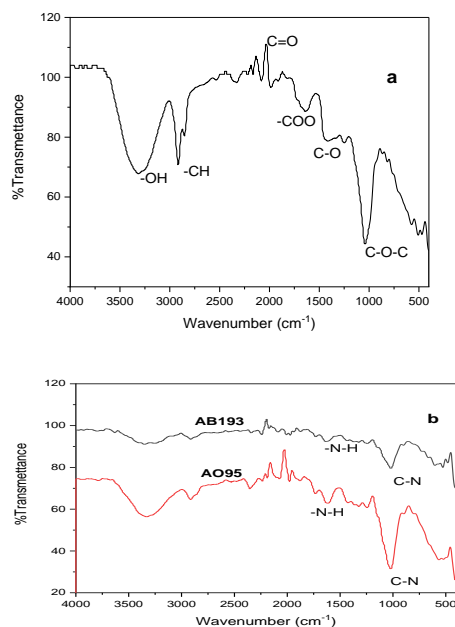


Fig. 6 : FTIR spectrum of dried watermelon peels (a) before adsorption and (b) after adsorption of AB193 and AO95

3.1.3 Scanning Electron Microscopy (SEM).

The surface morphology of DWP without any chemical treatment and its use as an environmentally friendly surface has been studied [21]. It can be seen from "Figure 7a" that the DWP consists of a very fine spherical shape, in addition to having a porosity which creates a large surface area to interact with the acidic dye molecules and enhance the adsorption. "Figure 7 b,c" , it clearly shows the accumulation of AB193 and AO95 particles on a surface DWP which proves that the adsorbent surface completely changed, pore sizes decreased and this indicates that AB193 and AO95 were successfully adsorbed on the surface of DWP.

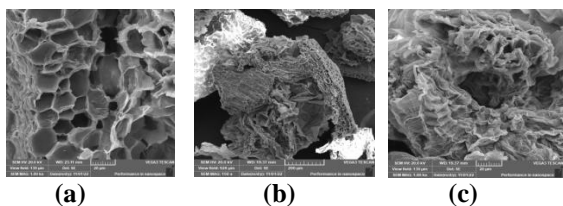


Fig. 7 : SEM image of dried watermelon peels (a) before adsorption ,(b) after adsorption AB193 and (c) after adsorption AO95 .

3.1.4 Energy-dispersive spectroscopy X-ray (EDX)

EDX analysis was used to clarify the qualitative elements composition of DWP before and after adsorption of AB193 by (a Quanta FEG 250 Czech Republic). As evidenced by X-ray spectroscopy, the composition of chemicals (in wt %) of DWP unloaded with AB193 was 48.57 for carbon and 51.43 for oxygen. Furthermore, the composition of chemicals (in wt %) of DWP loaded with AB193 was 33.73 for carbon, 61.26 for oxygen, 0.47 for nitrogen and 4.54 for sulfur as shown in "Figure 8 a,b " and Table 1 . Based on the noticeable differences in weight percent between DWP loaded and unloaded with AB193, it may be deduced that the AB193 molecules' successful adsorption on the pores of DWP caused a change in the chemical structure of the substance [22].

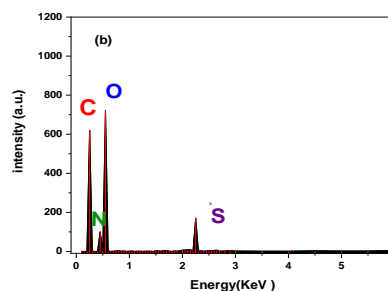
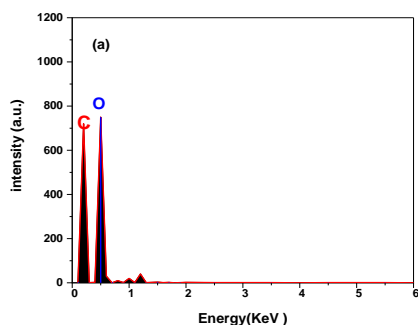


Fig. 8 : EDX analysis of dried watermelon peels (a) before adsorption and (b) after adsorption process.

Table 1 : Elemental composition of dried watermelon peels before and after adsorption process

Element %	Before adsorption	After adsorption
Carbon	48.57%	33.73%
Nitrogen	-	0.47%
Oxygen	51.43%	61.26%
Sulfur	-	4.54 %

3.2 Sorption of acid dyes from aqueous solution by agro-food waste dried watermelon Peels

In recent years, various adsorbents have been used to remove dye from polluted water [23]. DWP is one of the most effective and widely used adsorbents for dye removal from aqueous solutions. The development of novel approaches with simplicity, low cost and high efficiency is of great importance from theory and practice for wastewater treatment of dyes.

3.2.1 Effect of some parameter on sorption of dye

Using batch adsorption technique to study the effect of different experimental variables on dye absorption from water by agricultural food waste (dried watermelon Peels (DWP)), including the effect of pH, adsorbent doses, initial dye concentration, contact time and temperatures .

3.2.1.1 Effect of pH

The solution pH is one of the most important factors controlling the sorption of dyes onto adsorbent particles. In this work, adsorbent DWP was used to remove AB193 and AO95 dyes from aqueous solutions at various pH values from (3.0 to 10) as shown in" Figure 9 a,b". It was observed that the removal percent R % of DWP for acid dyes increased as pH decreased . This phenomenon can be explained by the following reasons ,the functional groups on DWP were protonated in the solution at a low pH. Thus, the electrostatic attraction between the positively charged DWP surface and the negatively

charged acidic dye in the solution increases the contact of the dye with DWP[24] . Besides, increasing the pH increased the negative charge density on a surface of DWP, which contributed to the lack of adsorption capacity[25] . Moreover, it is observed that the preferred absorption order of DWP for acidic dye and the maximum absorption of AB193 and AO95 dyes respectively are obtained at pH 3.0. Therefore a pH of 3 was chosen as the optimal pH for AB193 and AO95 dyes adsorption on DWP.

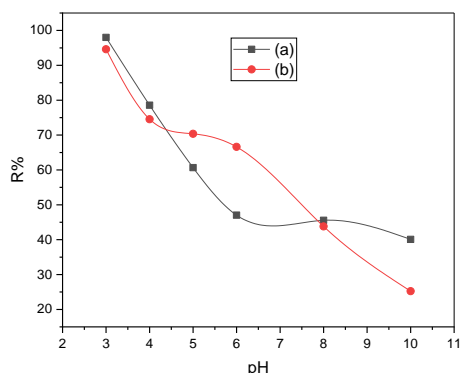


Fig. 9: Effect of pH on the adsorption of (a) AB193 and (b) AO95 dyes onto dried watermelon peels at [dose 0.3 g , dye conc. 50 ppm/20ml, t = 60 min. and 30°C].

3.2.1.2 Effect of dried watermelon peels (dosage)

Adsorbent dose represents an important parameter due to its strong effect on the capacity of an adsorbent at given initial concentration of adsorbate . The effect of adsorbent dose on the the removal percent of AB193 and AO95 dyes were conducted over a range of DWP doses of (0.01 to 0.4 g /20 ml at initial concentration of AB193 and AO95 dyes (50 Ppm) for contact time 60 min. at constant pH 3. The results are presented in "Figure 10 a,b " where , it is clearly observed that with increasing the adsorbent dose from 0.01 to 0.3 g , dye removal efficiency was increased from 36.33 to 97.99% for AB193 and from 28.12 to 95.51% for AO95 and then it become constant. The constancy in the removal percentage with increasing dose of adsorbent could be attributed to the increase of available adsorption surface and the availability of more adsorption sites. This stagnation constant in adsorption capacity with increasing dose of adsorbent is mainly due to the saturation of adsorption sites during the adsorption process[26,27] . Hence, (0.3 g) might be regarded as the ideal dose for DWP loading. There was no significant removal of dyes observed above the saturation point due to the establishment of equilibrium between the dye

molecules on the adsorbent and in the solution[28] .

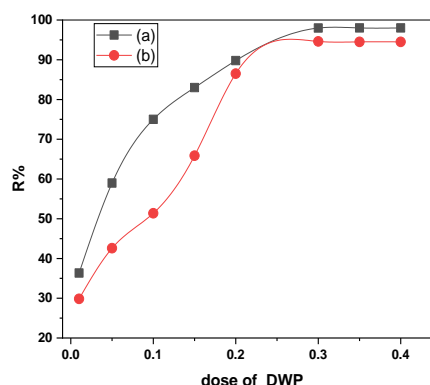


Fig. 10 : Effect of adsorbent dosage on the adsorption of (a) AB193 and (b) AO95 dyes onto dried watermelon peels at [pH= 3, dye conc. 50 ppm/20ml , t= 60 min. and 30°C].

3.2.1.3 Effect of dye concentration

The initial acid dyes concentration parameter was studied within the range (25–150 ppm) at 30 °C, pH 3, 0.3 g adsorbent dose, and 60 min contact time. From" Figure 11 a,b " When the initial concentration was increased up to 50 ppm, it was observed that the removal ratio R% sharply decreased, but after that, there were no noticeable changes in the removal ratio. This can be explained by the fact that at lower initial dye concentrations, there are more active sites on the surface of the adsorbent than at higher initial dye concentrations. So, At high concentrations of the initial acidic dye, the molecules have few opportunities for adsorption due to the limited number of binding sites on the surface of the adsorbent. As a result, some of the dye molecules are not absorbed and instead remain in the solution [29].

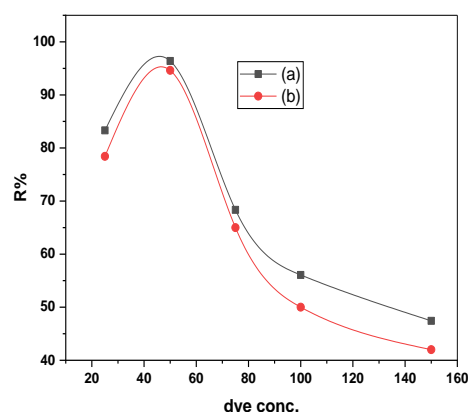


Fig. 9 : Effect of initial dye concentration on the adsorption of (a) AB193 and (b) AO95 dyes onto dried watermelon peels at [pH= 3 , dose 0.3 g ,t= 60 min. and 30°C].

3.2.1.4 Effect of contact time

The contact time of the adsorption process is an important parameter in the context of economic aspects of contaminated water treatment. The relationship between dye uptake and reaction time was studied for the uptake rate of dyes AB193 and AO95 by DWP. The contact time effects on the adsorption of the two acid dyes can be implemented by preparing the adsorbent solution using a fixed amount of 0.3 g of DWP in "Figure 12 a,b". In general, the adsorption rate of acidic dyes increases with the increase of contact time to a certain extent. A further increase in the contact time does not lead to an increase in the adsorption due to deposition of the dye on the available adsorption site on the adsorbent. The results indicate that the dye absorption rate increases depending on the contact time. In the first 30 min., the percentage of dye adsorption by the adsorbent is fast and after that it continues at a slower rate and finally reaches saturation at different contact time for initial concentration. The dye adsorption rate is initially higher due to the large surface area of the adsorbent DWP available for dye adsorption. After a certain period, only a very low increase in dye removal was observed because there were few active sites on the surface of the adsorbent. Then it reaches equilibrium at a point after which it becomes constant, because the surface of the adsorbent material becomes completely occupied, and the absorption capacity becomes constant [30]. Of the contact time studied, 60 min. of agitation time were detected to be sufficient to reach dye equilibrium.

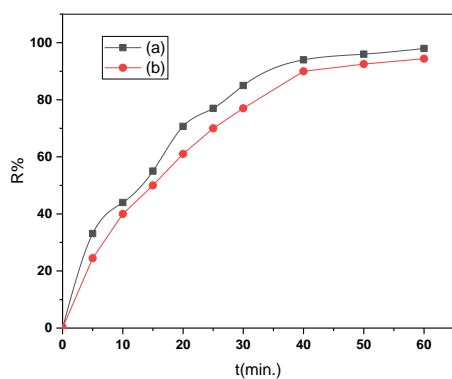


Fig. 12 : Effect of contact time on the adsorption of (a) AB193 and (b) AO95 dyes onto dried watermelon peels at [pH= 3 , dose 0.3 g , dye conc. 50 ppm/20ml and 30°C].

3.2.1.5 Effect of temperature

Most often, the temperature is utilised to determine whether a process is endothermic or exothermic. "Figure 13 a,b" shows how temperature affects an acidic media (pH =3) for adsorption of AB193 and AO95 dyes at 50 ppm on the surface of DWP with constant weight (0.3 g). It is clearly

shown that as temperature increased in the range (30–50 °C), the removal percent of AB193 and AO95 dyes decreased from 97.66% to 66.59% and from 94.84 % to 58.61 % respectively . This may be due to the physical bonds between the dye molecules and the active sites of the adsorbent that weaken with increasing temperature. Moreover, the solubility of the dye increases with temperature [31], and it is more difficult to absorb the solute because the forces between the solute and the solvent are higher than those between the solute and the adsorbent [32]. Moreover, it could result from a higher intrinsic viscosity of the solution [33,34].

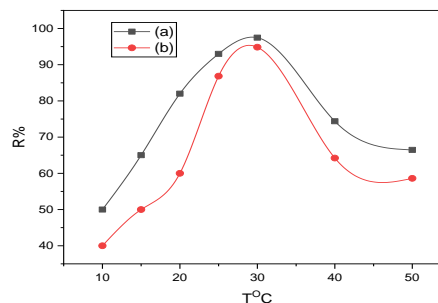


Fig. 13: Effect of temperature on the adsorption of (a) AB193 and (b) AO95 dyes onto dried watermelon peels at [pH= 3 , dose 0.3 g , dye conc. 50 ppm/20ml and t= 60 min].

Comparing the R% of AB139 and AO95 97.99 % and 95.51 % respectively on the DWP surface under the optimal conditions achieved in this study, it was found that the R% of AB139 was higher than that of AO95. This is due to the fact that the molecular size of the dye affects the absorption process because the particles of the adsorbent must enter the micropores of the adsorbent in order to be absorbed. A dense substance with a large molecular size reduces dye absorption [35].

3.3 Adsorption isotherm

The experimental data were fitted to the isotherm study using three isotherms (**Langmuir**, **Freundlich** and **Temkin**) models and use the correlation coefficients R^2 values, as indicated in "Table 2" to identify a practical model that can be used for design reasons.

3.3.1 Langmuir model

The Langmuir model describes monolayer sorption on distinct localized adsorption sites. It indicates no transmigration of the adsorbate in the plane of the surfaces and assumes uniform energies of monolayer sorption onto the sorbent surface [36]. C_e/Q_e versus C_e has a linear relationship as shown in "Figure 14 a,b", with a slope equal to $1/Q_m$ and an

intercept equal to $1/(Q_m K_L)$. The linear Langmuir equation is given as:

$$C_e/q_e = 1/(Q_m K_L) + C_e/Q_m \quad (2)$$

where “ Q_m ” is the maximum adsorption capacity (mg g^{-1}), and “ K_L ” is the Langmuir affinity constant (L mg^{-1}) related to “ Q_m ” and rate of adsorption. The feasibility of the process can be evaluated by a separation factor (dimensionless constant) “ R_L ” which is given in the following equation:

$$R_L = 1/(1 + (K_L C_0)) \quad (3)$$

The “ R_L ” value lays between zero and one for favorable adsorption, whereas ($R_L > 1$), ($R_L = 1$), and ($R_L = \text{zero}$) for unfavourable, linear, and irreversible adsorption respectively [37]. The values of the correlation coefficient for the Langmuir plots changed in the range 0.84 to 0.79. This suggests that the adsorption of AB 193 and AO95 onto the DWP did not follow the Langmuir model.

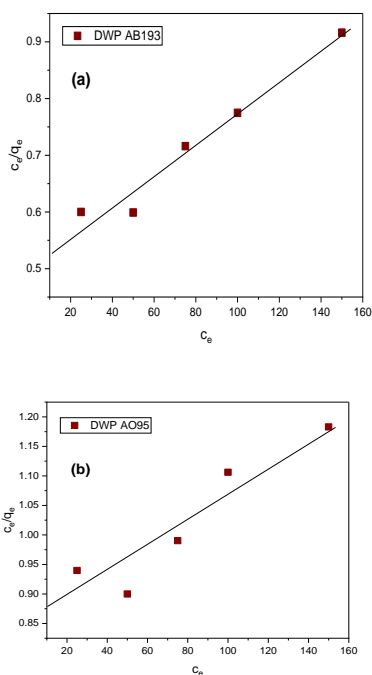


Fig. 14 : Langmuir adsorption isotherm of (a) AB193 and (b) AO95 dyes onto dried watermelon peels at [pH= 3 , dose 0.3 g , t= 60 min. and 30°C].

3.3.2 Freundlich model

The Freundlich isotherm is used to describe adsorption processes that occur on heterogeneous surfaces and active sites with different energies based on multilayer adsorption and equilibrium [38]. $\ln q_e$ versus $\ln C_e$ has a linear relationship as shown in “Figure 15 a,b”, with an intercept equal to $\ln K_f$ and a slope equal to $1/n$. The logarithmic form of Freundlich is given by the following equation:

$$\ln q_e = (1/n) \ln C_e + \ln K_f \quad (4)$$

where “ K_f ” is the Freundlich constant which represents the adsorption capacity of the adsorbent in (mg g^{-1}) and “ $1/n$ ” indicates the favourability of the adsorption process. The correlation coefficients ($R^2 > 0.99$) reflect that the experimental data agree well with the Freundlich model. The values of $1/n$ (0.71 and 0.85) are smaller than 1, so they represent the favorable adsorption conditions [39].

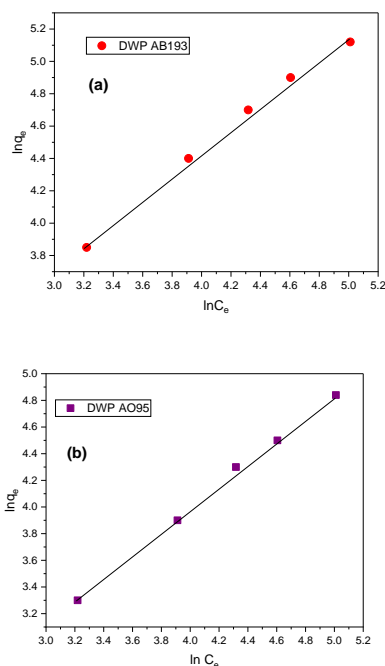


Fig. 15 : Freundlich adsorption isotherm of (a) AB193 and (b) AO95 dyes onto dried watermelon peels at [pH= 3 , dose 0.3 g , t=60 min. and 30°C].

3.3.3 Temkin model

Temkin's model is based on the hypothesis that the heat of adsorption due to interactions with the adsorbate decreases linearly with the recovery rate, whiting gas phase adsorption. This is an application of the Gibbs relation to the adsorbents, whose surface is considered homogeneous energy [40,41]. The equation for the Temkin model can be written as:

$$q_e = q_m \ln K_t + q_m \ln C_e \quad (5)$$

where K_t and q_m are the Temkin constants related to adsorption capacity in (L mg^{-1}) and heat of sorption in (J mol^{-1}) respectively [42]. The values of q_m and K_t can be obtained from the slope and intercept of the linear plot of q_e versus $\ln C_e$ as displayed in “Figure 16 a,b”.

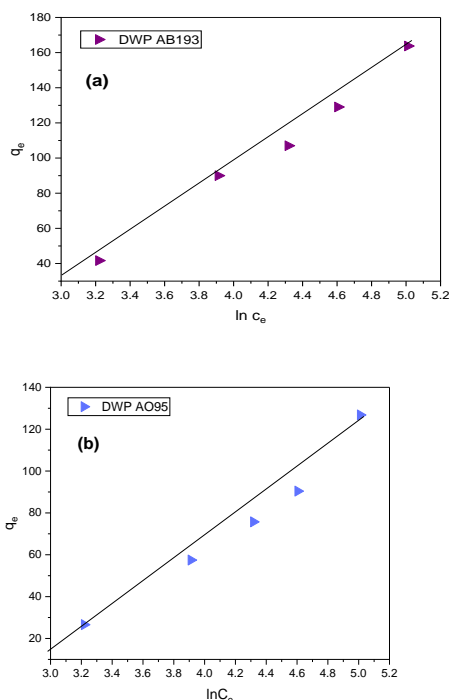


Fig. 16: Temkin adsorption isotherm of (a) AB193 and (b) AO95 dyes onto dried watermelon peels at [pH= 3 , dose 0.3 g , t= 60 min. and 30°C].

3.4 Kinetic study

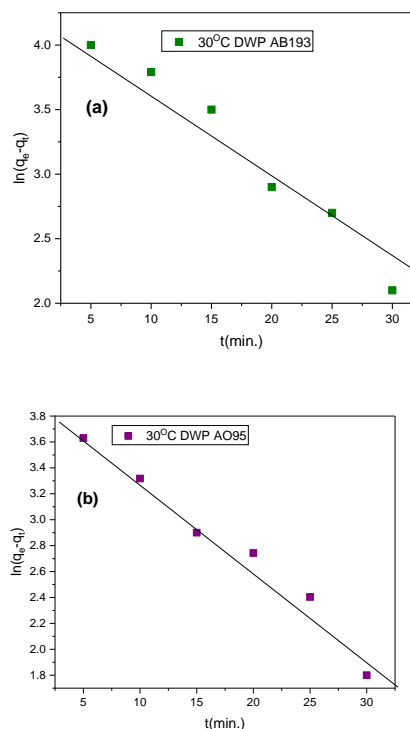


Fig. 17: First- order kinetic model for adsorption of (a)AB193 and (b) AO95 onto dried watermelon peels at [pH= 3 , dose 0.3 g , dye conc. 50 ppm/20ml ,t = 60 min. and 30°C].

Table 2 : Langmuir, Freundlich and Temkin isotherm constants of adsorption of AB193 and AO95 dyes onto dried watermelon peels at 30 °C .

Dye type	Langmuir adsorption isotherm				Freundlich adsorption isotherm			Temkin adsorption isotherm		
	Q_{max} (mg/g)	$k_L \times 10^{-2}$ L (mg^{-1})	$R_L \times 10^4$	R^2	K_F (dm^3g^{-1})	1/n	R^2	q_m	K_t	R^2
AB 193	369	1.85	2.16	0.84	5.07	0.71	0.99	65.94	0.074	0.97
AO 95	434	3.65	1.09	0.90	1.85	0.85	0.99	53.63	0.060	0.96

Four kinetic models [The pseudo-first-order , the pseudo-second-order , The intra-particle diffusion , The Elovich model] were used to fit the experimental data at 50 ppm initial dye concentration using a linear regression analysis method. The parameters of these models are summarized in "Table 3". The pseudo-first-order rate expression is given as: [43,44]

$$\log(q_e - q_t) = \log(q_e) - k_1 t / 2.303 \quad (6)$$

where q_t is the amount of dye adsorbed on the adsorbent at any time, t in (mgg^{-1}), and k_1 is the first-order rate constant. A "Figure 17 a,b" of $\log(q_e - q_t)$ versus t gives a linear relationship from which the value of k_1 and q_e can be determined from the slope and intercept.

The linearized form of the pseudo-second-order model is given as: [45,46]

$$t/q_t = (1/(k_2(q_e^2))) + t / q_e \quad (7)$$

where k_2 is the rate constant of the pseudo-second-order adsorption. The plot of t/q_t versus t in "Figure 18 a,b" gives a linear relationship from which q_e and k_2 can be determined from the slope and intercept of the plot respectively. The correlation coefficients R^2 higher than 0.99 suggest that adsorption of AB193 and AO95 onto DWP predominantly follows the pseudo-second order kinetic model [47].

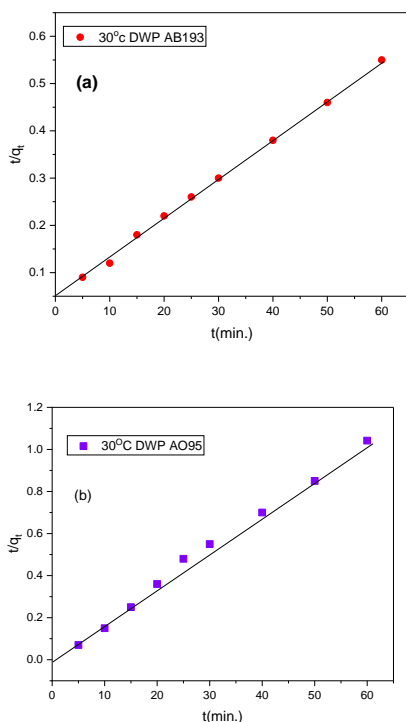


Fig. 18: Second- order kinetic model for adsorption of (a) AB193 and (b) AO95 onto dried watermelon peels at [pH= 3 , dose 0.3 g , dye conc. 50 ppm/20ml , t = 60 min. and 30°C].

The intra-particle diffusion model used based on the following Equation: [48]

$$q_t = k_p t^{1/2} + C \quad (8)$$

Where q_t (mg/g) is the amount of dye adsorbed at time t , K_p (mg/g min^{1/2}) is the intra-particle diffusion rate constant obtained from the slope, of the plot q_t versus $t^{1/2}$ as shown in “Figure 19 a,b”. While the C value gives an indication of the thickness of the boundary layer. The larger C shows greater boundary layer effect that account greater contribution of the surface sorption in the rat-limiting step [49]. This kinetic study confirmed that sorption of AB193 and AO95on DWP was a multi step process, involving in sorption on the external surface and diffusion into the interior with external surface chemical sorption being the rate- controlling step.

The Elovich model is generally expressed as:

$$q_t = 1/\beta \ln(\alpha\beta) + 1/\beta \ln t \quad (9)$$

Where α is the initial adsorption rate constant (mg/(g min)) and the parameter β is the desorption constant (g / mg) . The constant can be obtained from the slope and the intercept of the plot of q_t versus $\ln t$, as shown in “Figure 20 a,b” gives a linear relationship

with a slope of “ $1/\beta$ ” and an intercept of $1/\beta \ln(\alpha\beta)$ [50] .

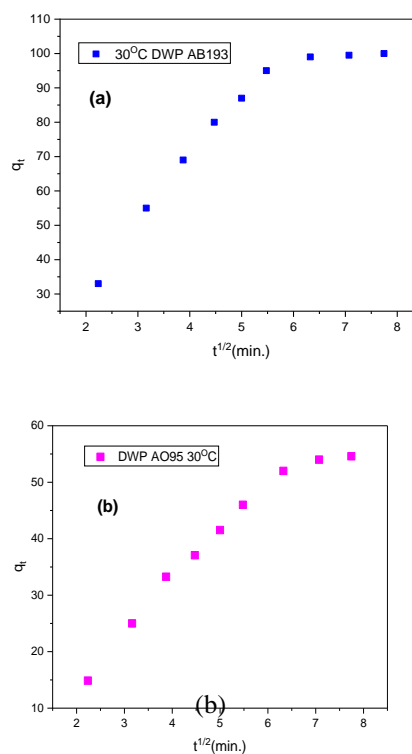


Fig. 19: Intra-particle diffusion model for adsorption of (a) AB193 and (b) AO95 dyes onto dried watermelon peels at [pH= 3 , dose 0.3 g , dye conc. 50 ppm/20ml , contact time 60 min. and 30°C].

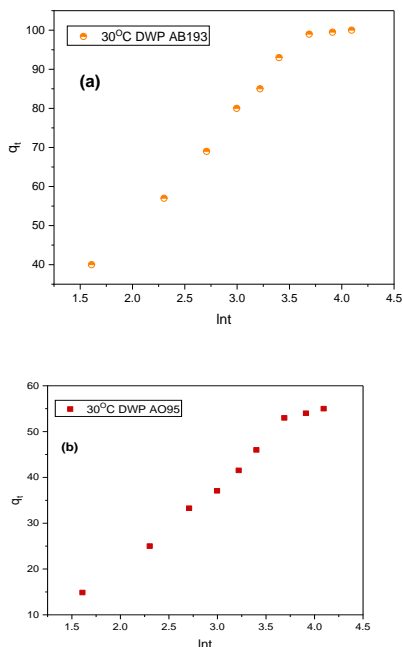


Fig. 20: Elovich kinetic model for adsorption of (a) AB193 and (b) AO95 onto dried watermelon peels at at [pH= 3 , dose 0.3 g , dye conc. 50ppm/20ml ,t= 60 min. and 30°C].

Table 3: Kinetics parameters of (a) AB193 and (b) AO 95 dyes onto dried watermelon peels .

Dye Type	Te. (°C)	Pseudo first-order model		Pseudo second-order model		Intraparticle Diffusion model			Elovich equation model		
		$k_1 \times 10^2$ (min ⁻¹)	R ²	$K_2 \times 10^4$ (g/mg min)	R ²	K_p mg/g min ^{-1/2}	C (mg g ⁻¹)	R ²	A (mg(g min ⁻¹))	$\beta \times 10^2$ (g mg ⁻¹)	R ²
AB193	30	8.42	0.90	16.32	0.99	16.65	6.950	0.99	22.32	3.50	0.99
AO95	30	6.67	0.89	18.14	0.99	18.14	-15.20	0.99	8.43	5.49	0.99

3.5 Thermodynamic study

To establish a criterion for determining the feasibility or spontaneity of the adsorption process the chemical thermodynamic parameters had been examined. The enthalpy ΔH^0 and entropy ΔS^0 were calculated using Equation (10):

$$\ln K_c = \Delta S^0/R - \Delta H^0/(RT) \quad (10)$$

"Figure 21" and the table 4 show the removal of AB193 and AO95 with increasing temperature from 283 to 303 . However, the removal of dyes decreases with the increase in temperature beyond 303 K.

The observation can be attributed to the weakening of bonds between the dye molecules and active sites of DWP at high temperatures that may lead to the decreased surface active sites as well as adsorption capacity [51]. The negative value of ΔH^0 - 0.064, -0.041 k J mol⁻¹ confirmed the exothermic nature of the adsorption process confirming that physical forces occur during the adsorption of AB193 and AO95 onto DWP respectively. This is in good agreement with n value derived from Freundlich isotherm.

The negative value of ΔS^0 -0.024 and -0.018 k J mol⁻¹K⁻¹ entropy for AB193 and AO95 respectively revealed the decrease in the randomness at solid–solution interface through the adsorption of AB193 and AO95 onto DWP. This indicates that adsorption leads to an increase in the dyes order at the solid–liquid interface during the adsorption process on DWP and is supportive of the interaction between two dyes and DWP. As the temperature increases, the mobility of dyes molecules increases causing the ions to escape from the solid phase to the liquid phase [52].

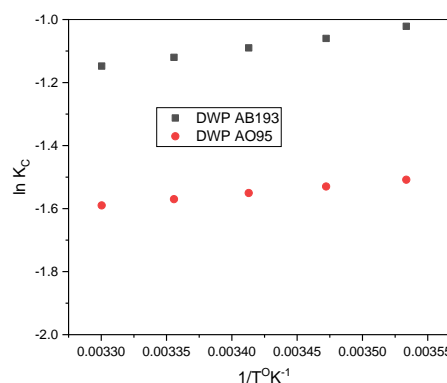
Table 4: Thermodynamic parameters for the adsorption of AB193 and AO95 onto dried watermelon peels.

Dye type	Temp. 0C	Temp. 0K	ΔH^0 (kJ/mol)	ΔS^0 (KJ/mol)	ΔG^0 (kJ/mol)
AB193	10	283	-0.064	-0.024	6.72
	15	288			6.84
	20	293			6.96
	25	298			7.08
	30	303			7.20
AO95	10	283	-0.041	-0.018	5.05
	15	288			5.14
	20	293			5.23
	25	298			5.27
	30	303			5.41

Gibbs free energy change, ΔG^0 , can be calculated in terms of enthalpy and entropy as in the following Equation (11) [50,51].

$$\Delta G^0 = \Delta H^0 - T \Delta S^0 \quad (11)$$

which gives positive values at all temperatures so, the adsorption of AB193 and AO95 onto dried watermelon peels DWP is physisorption because the free energy values fall in the range of (48 to 0 kJ mol⁻¹). Hence, the links between dye molecules and the adsorbent surface can be due to vander Waals or electrostatic attraction forces [53].

**Fig. 21: Variation of $\ln K_c$ with $1/T$ (K⁻¹) for estimation of the enthalpy and entropy for the adsorption of AB193 and AO95 onto dried watermelon peels .**

4. Conclusion

The results of this study indicate that dried watermelon peels can be used as a bio-sorbent material with great potential to remove various pollutants in addition to its low cost to remove acid dyes. The successful result demonstrates the possibility of using dried watermelon peels (DWP) as an effective adsorbent to remove acid dyes from aqueous solution. The best removal efficacy was reported at pH = 3, 60 min. Contact duration, 0.3 g adsorbent dose, and dye concentration 50 ppm, indicating that acidic conditions improved the percentage of acidic dye removal. The Freundlich model, which explains multilayer adsorption on heterogeneous surfaces, best fits the adsorption process. Additionally, the dye uptake rate constants based on fictitious second order kinetic models. In contrast to the negative values of ΔH^0 and ΔS^0 , which demonstrate that the reaction is exothermic and that the solubility of the dye molecules increases with increasing temperature, positive values of ΔG^0 demonstrate that the process is physical and non-spontaneous adsorption at low temperatures. As a result, the removal ratio decreases.

5. Conflicts of interest

There are no conflicts to declare.

6. Formatting of funding sources

No funding sources.

Reference

- [1] Mansoorian H.J., Mahvi A.H. and Alizade M., Equilibrium and synthetic studies of methylene blue dye removal using ash of walnut shell, *J. Health Field*, 2013, 1(3):38–45.
- [2] Tang R., Dai C., Li C., Liu W., Gao S. and Wang C., Removal of methylene blue from aqueous solution using agricultural residue walnut Shell: equilibrium, kinetic, and thermodynamic studies, *J. of Chem.*, 2017: 1-10.
- [3] Bonetto L.R., Crespo J.S., Guégan R., Esteves V.I., Giovanela M., Removal of methylene blue from aqueous solutions using a solid residue of the apple juice industry: Full factorial design, equilibrium, thermodynamics and kinetics aspects, *Journal of Molecular Structure*, 2021,1224(15):129296.
- [4] Aseel M. Aljeboree, A.F.A., Role of plant wastes as an ecofriendly for pollutants (Crystal Violet dye) removal from aqueous solutions, *Plant Archives*, 2019, 19(2): p 902-905.
- [5] Hoppen, M.I., et al., Adsorption and desorption of acetylsalicylic acid onto activated carbon of babassu coconut mesocarp., *Journal of Environmental Chemical Engineering*, 2019, 7(1): p 102862.
- [6] Wenyan Jiang, L.Z., Xiaoming Guo, Mei Yang, Yiwen Lu, Yijun Wang, Yousen Zheng and Guangtao Wei, Adsorption of cationic dye from water using an iron oxide/ activated carbon magnetic composites prepared from sugarcane bagasse by microwave method., *Environmental Technology*, 2019, 2 : 10.1080/ 09593330.
- [7] Qusay K. Mojar Alshamusi, A.A.M.A., Makarim A. Mahdi, Layth S. Jasim and Aseel M. Aljeboree, Adsorption of Crystal Violet (CV) Dye in Aqueous Solutions by Using P(PVP-CO-AAM)/ GO Composite as (eco- healthy adsorbate surface) : Characterization and thermodynamics studies, *Biochem. Cell. Arch.*, 2021, 12 : 2423-2431.
- [8] Rafid Q. K., Aseel M. A., Layth S. J., Ayad F. A., Synthesis and identification of Azo Disperse dye derived from 4-Aminoantipyrine and their applications to determine some drugs, *International Journal of Drug Delivery Technology*, 2021, 11(3) : 1040-1044.
- [9] Aseel M. A., Ali L. and Hanadi M. A., Photocatalytic degradation of textile dye cristal violet wastewater using zinc oxide as a model of pharmaceutical threat reduction, *Journal of Global Pharma Technology*, 2019, 11(02): 138-143.
- [10] Aseel M., Aljeboree I.J.S., Layth S. J., Ayad F. A., Introducing a novel chemical method of treatment for dye removal : Removal of maxillon blue and direct yellow from aqueous solution, *Caspian Journal of Environmental Sciences*, 2021, 19(4): 673-684.
- [11] Shoomaila L., Rabia R., Muhammad I., Shahid I., Ayesha K. and Liviu M., Removal of Acidic Dyes from Aqueous Media Using Citrullus Lanatus Peels: An Agrowaste-Based Adsorbent for Environmental Safety, *Hindawi Journal of Chemistry*, 2019, 6704953:1-9
- [12] Enniya I., Jourani A., Study of Methylene Blue Removal by a biosorbent prepared with Apple peels, *Journal of Materials and Environmental Sciences*, 2017, 8 (12): 4573-4581.
- [13] Padmesh T.V.N., Vijayaraghavan K., Sekaran G., Velan M., Batch and column studies on biosorption of acid dyes on fresh water macro alga *Azolla filiculoides*, *Journal of Hazardous Materials* 2005,(125):121-9.
- [14] Nemr A.E., Potential of pomegranate husk carbon for Cr(VI) removal from wastewater: Kinetic

and isotherm studies., *Journal of Hazardous Materials*, 2009 ,(161):132-41.

[15]Zazouli M.A., Yazdani J., Balarak D., Ebrahimi M., Mahdavi Y., Removal Acid Blue113 from Aqueous Solution by Canola, *Journal of Mazandaran University Medical Science*, 2013,23(2):73-81.

[16] Ali H., Jawad Y. S. & Khairul A. R., Utilization of watermelon (*Citrullus lanatus*) rinds as a natural low-cost biosorbent for adsorption of methylene blue: kinetic, equilibrium and thermodynamic studies, *Journal Of Taibah University Science*, <https://doi.org/10.1080/16583655.2018.1476206>.

[17] Uner O., Gecgel U., Bayrak Y. ,Preparation and characterization of mesoporous activated carbons from waste watermelon rind by using the chemical activation method with zinc chloride, *Arab J Chem.* ,2019, 12 (8): 3621-3627.

[18] Zhang, M. P., LandryP. W. Barone et al., *Molecular* recognition using corona phase complexes made of synthetic polymers adsorbed on carbon nanotubes, *Nature Nanotechnology*, 2013,8, (12): 959–968.

[19] Aseel M. , , Ghadeer S. H., Ayat A. K., Mohammed M.A., Holya A. L., Aiman M. B. Al., Ayad F. A. and Salwan A. A., Highly adsorption surface from watermelon peels : as non-conventional low cost sorbent ; Equilibrium and Recyclestudy , *Earth and Environmental Science* , 2022, 1029 :012008.

[20] Mansour R., Sameda M. G. and Zaatout A., Adsorption studies on brilliant green dye in aqueous solutions using activated carbon derived from guava seeds by chemical activation with phosphoric acid, 2020,202 :396–409.

[21] Ashish S., Aniruddha M., Vikas V., Prakash D., Mansing A., Sanjay S., Removal of malachite green dye from aqueous solution with adsorption technique using limonia acidissima (wood apple) shell as low cost adsorbent, *Arabian Journal of Chemistry*, 2017 , 10 :3229-3238.

[22] Ramadan A.M., Mohamed G. S.and Ahmed A.Z., Removal of brilliant green dye from synthetic wastewater under batch mode using chemically activated date pit carbon, *R.S.C. Adv.*, 2021, 11, 7851.

[23] Shahat A., Hassan H.M.A., Azzazy H.M.E., El-Sharkawy E.A., Abdou H.M. and Awual M.R., Novel hierarchical composite adsorbent for selective lead(II) ions capturing from wastewater samples, *Chem. Eng. J.* , 2018, 332:377–386.

[24] Mansour R. A., Aboeleneen N. M. and Abdelmonem N. M., Adsorption of cationic dye from aqueous solutions by date pits: Equilibrium, kinetic, thermodynamic studies, and batch adsorber design, *Int.J. Phytorem.*, 2018, 20:1062–1074.

[25] Mahmoud A.S., Abdel E. G. and Brooks M.S., Removal of Dye from Textile Wastewater Using Plant Oils Under Different pH and Temperature Conditions, *Am. J. of Env. Sci.*, 2007,3(4) :205-218.

[26] Ali S. , A review on adsorbent parameters for removal of dye products from industrial wastewater, *Water Quality Res. J.*, 2021,56(4):181.

[27] Aseel M. A., Ghadeer S. H., Ayat A. K., Mohammed M. A., Holya A. L., Aiman M. B., Ayad F. A. and Salwan A. A. ,Highly adsorbent surface from watermelon peels : as non-conventional low-cost sorbent ; Equilibrium and Recycle study, 2022, DOI 10.1088/1755-1315/1029/1/012008.

[28] Lakshmipathy R., Sarada N.C., Adsorptive removal of basic cationic dyes from aqueous solution by chemically protonated watermelon (*Citrullus lanatus*) rind biomass, *Desalination and Water Treatment*, (2013) :1–10.

[29] Saif M., Rehman U., Munir M., Ashfaq M. and Rashid N., Adsorption of Brilliant Green dye from aqueous solution onto red clay, *Chem. Eng. J.*, 2013, 228:54–62.

[30] Khaniabadi Y.O., Mohammadi M.J., Shegerd M., Sadeghi S., Saeedi S. and Basiri H., Removal of Congo red dye from aqueous solutions by a low-cost adsorbent: activated carbon prepared from Aloe vera leaves shell, *J. Env. Health Eng. and Manage*, 2017, 4:29-35

[31] Abdel A.K.M., Francis R .M., Exploring the adsorption behavior of cationic and anionic dyes on industrial waste shells of egg, *J Environ Chem Eng*, 2017,5(1):319–27.

[32] Obaid M.H. ,Thermodynamic study of adsorption cationic methylene blue dye on the plant residue., *Kufa J Chem.*, 2011,2:55–63

[33] Pekel N., Güven O., Solvent, temperature and concentration effects on the adsorption of poly (n-butyl methacrylate) on alumina from solutions ,*Turk J Chem.*, 2002,26(2):221–8.

[34]. Manna S., Roy D., Saha P., Gopakumar D., Thomas S., Rapid methylene blue adsorption using modified lignocellulosic materials, *Process Saf Environ Prot.*, 2017,107:346–56.

- [35]. Hossam A., Tarek E. K., and Reda A., The effect of dye chemical structure on adsorption on activated carbon: a comparative study, *Society of Dyers and Colourists, Color. Technol.*, 2014, 130: 205–214.
- [36] Alice S. C., José D. F., David L. N. and Sandra M. D., Removal of textile dye by adsorption on the cake as solid waste from the press-extraction of the macaúba (*Acrocomia aculeata*) kernel oil, *Eclética Química*, 2018, 43 (1) : 48-53 .
- [37] Edet U.A., Ifelebuegu A.O. ,Kinetics, isotherms, and thermodynamic modeling of the adsorption of phosphates from model wastewater using recycled brick waste, *Processes*,2020,8(6):665.
- [38] Saruchi A. and Vaneet K., Adsorption kinetics and isotherms for the removal of rhodamine B dye and Pb^{+2} ions from aqueous solutions by a hybrid ion-exchanger, *Arab. J of Chem.* , 2019, 12(3):316-329.
- [39] Riham E., Elshimaa H. Gomaa, Heba E. ,Amina E., Nagwa B., Dyeing of Waste Cotton Fabric as Biosorbent of Heavy Metals from Aqueous Solution, *Egypt. J. Chem.*, 2022,65(2):377 - 387.
- [40].Diyanati R.A., Yousefi Z., Cherati J.Y., Balarak D., Adsorption of phenol by modified azolla from Aqueous Solution ,*Journal of Mazandaran University of Medical Science*, 2013,22(2):13-21.
- [41] Hossain M.A., Ngo H.H., Guo W., Nguyen T.V., Removal of copper from water by adsorption onto banana peel as bioadsorbent, *Int. J. Geomate*, 2012,2: 227–234.
- [42]Zazouli M.A., Balarak D, Karimnejhad F., Kinetics modeling and isotherms for adsorption of fluoride from aqueous solution by modified lemna minor, *Journal of Mazandaran University of Medical Science*, 2013,23:106.
- [43] Silva L.P., Pereira T.M., Bonatto C.C., Frontiers and perspectives in the green synthesis of silver nanoparticles. In *Green synthesis, characterization and applications of nanoparticles* ,2019 :137-164.
- [44] Moussout H. , Ahlafi H. , Aazza M. and Maghat H., Critical of linear and nonlinear equations of pseudo-first order and pseudo-second order kinetic models ,*Int. J. of Modern Sci.* , 2018, 4, 244:254.
- [45] Naderi P. , Shirani M. , Semnani A. and Goli A. , Efficient removal of crystal violet from aqueous solutions with *Centaurea* stem as a novel biodegradable bioadsorbent using response surface methodology and simulated annealing: Kinetic, isotherm and thermodynamic studies, *Ecotoxicology and Env. Safety*, 2018, 163:372-381
- [46] Chen Y., Zhang D., Adsorption kinetics, isotherm and thermodynamics studies of flavones from *Vaccinium Bracteatum* Thunb leaves on NKA-2 resin, *Chemical Engineering Journal*, 2014 ,15,254:579-85.
- [47] Mostafa R.i K. Z., Moradi O., Sillanp M., Abdullah V. K. G., Asiri M. and Agarwal S., A review on removal of uranium(VI) ions using titanium dioxide based sorbents,*J. Mol. Liq.*, 2019, 293, 111484.
- [48] Yuan X., Xia W., An J., Yin J., Zhou X. and Yang W., Kinetic and Thermodynamic Studies on the Phosphate Adsorption Removal by Dolomite Mineral, *J. Chem.*, 2015:1–8 .
- [49] Shahwan T. ,Sorption kinetics: obtaining a pseudo-second order rate equation based on a mass balance approach.,*Journal of Environmental Chemical Engineering*, 2014 ,2(2):1001-6.
- [50] Ghasemi N., Tamri P., Khademi A., Nezhad N.S., Alwi S.R., Linearized equations of pseudo secondorder kinetic for the adsorption of Pb (II) on pistacia atlantica shells, *Ieri Procedia.*, 2013 ,1,5:232-7.
- [51] Tserendulam S., Yu G., Nadmid G., Kh S.U. ,Studies of kinetics and thermodynamic parameters of cashmere dyeing with bio-preparation of *Urtica Cannabina* L., *Proceedings of the Mongolian Academy of Sciences*, 2019, 26:4-15.
- [52] Gohr M.S., Abd-Elhamid A.I., El-Shanshory A.A., Soliman H.M., Adsorption of cationic dyes onto chemically modified activated carbon: Kinetics and thermodynamic study., *Journal of Molecular Liquids*, 2022 , 15,346:118227.
- [53] Nurul I. T.Nur A. R., Nurul I. S., Nyliawani M. R., Nur Amalin A.K., Nadhirah N. T. A., Kinetic, equilibrium, and thermodynamic studies of untreated watermelon peels for removal of copper(II) from aqueous solution, *Desalination and Water Treatment*, 2021, 227 : 289–299.